Toxicology Letters 228 (2014) 207–215

Contents lists available at ScienceDirect

Toxicology Letters

journal homepage: www.elsevier.com/locate/toxlet

Effects of PAMAM dendrimers in the mouse brain after a single intranasal instillation

Tin-Tin Win-Shwe[a], Hideko Sone[b,*], Yoshika Kurokawa[b], Yang Zeng[b], Qin Zeng[b], Hiroshi Nitta[a], Seishiro Hirano[b]

[a] Center for Environmental Health Sciences, National Institute for Environmental Studies, 16-2 Onogawa, Tsukuba, Ibaraki 305-8506, Japan
[b] Center for Environmental Risk Research, National Institute for Environmental Studies, 16-2 Onogawa, Tsukuba, Ibaraki 305-8506, Japan

HIGHLIGHTS

- A single dose of PAMAM dendrimers was intranasally administered to 8-week old male BALB/c mice.
- Gene expression profiling was examined in the olfactory bulb, hippocampus, and cerebral cortex of the mouse brain.
- Brain derived-neurotrophic factor mRNA was up-regulated in the hippocampus and cerebral cortex in PAMAM-treated mice.
- PAMAM dendrimers may reach the brain after intranasal instillation and induce neuronal effects.

ARTICLE INFO

Article history:
Received 28 October 2013
Received in revised form 20 April 2014
Accepted 22 April 2014
Available online 9 May 2014

Keywords:
Nanomaterials
PAMAM dendrimers
Biomarkers
Neurotoxicity
Mouse

ABSTRACT

Dendrimers are highly branched spherical nanomaterials produced for use in diagnostic and therapeutic applications such as a drug delivery system. The toxicological profiles of dendrimers are largely unknown. We investigated the *in vivo* effects of nasal exposure to polyamidoamine (PAMAM) dendrimers on their effects on neurological biomarkers in the mouse brain. A single dose of PAMAM dendrimers (3 or 15 μg/mouse) was intranasally administered to 8-week old male BALB/c mice. Twenty-four hours after administration, the olfactory bulb, hippocampus, and cerebral cortex were collected and potential biomarkers in the blood and brain were examined using blood marker, microarray and real-time RT-PCR analyses. No remarkable changes in standard serum biochemical markers were observed in the blood. A microarray analysis showed the alterations of the genes expression level related to pluripotent network, serotonin-anxiety pathway, TGF-beta receptor signaling, prostaglandin synthesis-regulation, complement-coagulation cascades, and chemokine-signaling pathway and non-odorant GPCR signaling pathways in brain tissues. Brain derived-neurotrophic factor mRNA was up-regulated in the hippocampus and cerebral cortex in mice treated with a high dose of dendrimers. These findings suggest that PAMAM dendrimers may reach the brain *via* the systemic circulation or an olfactory nerve route after intranasal instillation, and indicate that a single intranasal administration of PAMAM dendrimers may potentially lead to neuronal effects by modulating the gene expression of brain-derived neurotrophic factor signaling pathway.

1. Introduction

Dendrimers are generally described as macromolecules with highly branched structures that provide a high degree of surface functionalities and interior cavities. Dendrimers are very promising nanomaterials for therapeutic and diagnostic purposes (Lee et al., 2005; Tekade et al., 2009). Because of their multivalent and monodisperse characters, dendrimers have been a topic of interest in the fields of chemistry and biology, especially for applications in drug delivery, gene therapy, and chemotherapy (Buhleier et al., 1978; Newkome et al., 1985; Tomalia et al., 1985). Current understanding of the toxicological and pharmacological effects of dendrimers is limited, and an improved understanding of the toxicities of various dendrimer formulations is essential. Toxicological and pharmacokinetic investigations examining the cytotoxicity of dendrimers and the immune response to dendrimers are needed

* Corresponding author. Center for Environmental Risk Research National Institute for Environmental Studies 16-2, Onogawa, Tsukuba, Ibaraki 305-8506, Japan Tel.: +81 29 850 2464; fax: +81 29 850 2546.
E-mail address: hsone@nies.go.jp (H. Sone).

http://dx.doi.org/10.1016/j.toxlet.2014.04.020
0378-4274/

to design dendrimers for therapeutic and diagnostic uses. Although attention has been paid to clinical applications, little is known about their biological safety. Therefore, the possible adverse effects on humans and the environment needed to be evaluated.

Nanoparticles are divided into combustion-derived nanoparticles and manufactured or engineered nanoparticles. Previously, our laboratory has demonstrated the effects of the intranasal instillation of carbon black nanoparticles on inflammatory mediators in the mouse brain (Win-Shwe et al., 2006) and the effects of inhalation exposure to nanoparticle-rich diesel exhaust on the expression level of memory function-related genes and hippocampal dependent spatial and non-spatial learning behavior (Win-Shwe et al., 2008a, 2009, 2012a, 2012b; Win-Shwe et al., 2011). Nanotechnology has been advanced increasingly and among the well-developed nanomaterials, polyamidoamine (PAMAM) dendrimers are widely used for various biomedical applications including drug delivery, molecular imaging, and gene therapy (Na et al., 2006; Zhou et al., 2006; Dear et al., 2006; Swanson et al., 2008). PAMAM dendrimers are synthesized using a divergent method starting from ammonia or ethylenediamine initiator core reagents (Pushkar et al., 2006). Currently, many *in vitro* studies using mammalian cell lines have shown the cytotoxicity of PAMAM dendrimers (Lee et al., 2009; Naha et al., 2010; Mukherjee et al., 2010a, 2010b). It was reported that PAMAM dendrimers can make a hole in the plasma membrane, which may trigger membrane disruption (Hong et al., 2004; Leroueil et al., 2008). Toxicity has also been shown to increase with increasing dendrimer generation (Naha et al., 2009). However, reports describing the *in vivo* toxicological assessment of dendrimers are limited. These findings prompted us to investigate the toxicological effects of dendrimers.

Regarding recent *in vivo* studies of nanomaterials, the intranasal instillation of titanium dioxide nanoparticles for 90 consecutive days was reported to induce oxidative stress and to trigger the overproliferation of spongiocytes and to induce hemorrhage in the mouse brain (Ze et al., 2013). Moreover, a kinetic study has reported that zinc oxide nanoparticles have a higher absorption and a more extensive organ distribution, compared with titanium dioxide nanoparticles, after 13 weeks of oral exposure (Cho et al., 2013).

We hypothesized that since dendrimers are nano-sized particles, they could potentially reach the brain *via* an olfactory nerve or through the systemic circulation following intranasal instillation, as previously described in our other studies (Win-Shwe et al., 2006, 2008b); once they have reached the brain, they might affect the immune system or induce an inflammatory response. Therefore, we selected the olfactory bulb to detect the effects of intranasally instilled dendrimers. Other areas, such as the hippocampus and the cerebral cortex, were selected to enable a comparison with our previous findings for neuro-immune biomarkers in those areas after the intranasal instillation of nanoparticle carbon black. Therefore, in the present study, to determine whether PAMAM dendrimers cause toxicity in an animal model, we used male BALB/c mice to assess the neurotoxic effects of the single intranasal administration of PAMAM dendrimers on neurological biomarkers in the mouse brain. We also assessed the genes affected by PAMAM dendrimers using microarray analyses.

2. Materials and methods

2.1. Nanomaterials

PAMAM dendrimer (1,4-diaminobutane core, generation 4, 10% w/w methanol solution) was purchased from Sigma–Aldrich (product number 683507, PAMAM-amine dendrimer, NH_2 surface type, positive charge; St. Louis, MO, USA). The dendrimer particles were desiccated after the spontaneous volatilization of methanol and were re-suspended in ultrapure water (Milli-Q). Aliquots were then used in the experiments after storage for more than one day to enable a thorough distribution of the particles.

2.2. Characterization of PAMAM-NH_2 dendrimers

According to the manufacturer, the primary size of PAMAM-NH_2 dendrimers (G4) is 4.5 nm in diameter; each dendrimer has 64 (amine) surface groups and a molecular weight of 14,234 Da. A schematic diagram of the PAMAM dendrimer (G4) that was used in the present study and the distribution of the hydrodynamic diameter of PAMAM dendrimers in ultrapure water are shown in Fig. 1. In the present study, we selected G4 dendrimers because our *in vitro* pilot study had shown that among the PAMAM dendrimers, the G4 dendrimers were associated with potential cytotoxicity in human neural progenitor cells. The particle size distributions were calculated using the light intensity distribution data. For measurement, the whole range of operations from the detection of scattered light intensity distribution patterns to the calculation of the particle size distribution was performed. Using Zeta Potential and Particle Analyzer (Otsuka Electronics ELSZ-2, Osaka, Japan) we first measured the particle size distribution of PAMAM in 100% methanol (mean size, 3.4 ± 0.9 nm); after removing methanol using nitrogen purging, PAMAM was again distributed in ultrapure water (mean size, 5.7 ± 1.4 nm in first peak; 976 ± 391 nm in second peak). Then, the PAMAM was stored in ultrapure water overnight to allow the thorough dispersal of the PAMAM dendrimers (mean size, 5.6 ± 2.3 nm; second peak was disappeared) prior to use in the intranasal instillation experiments.

2.3. Animals

Male BALB/c mice (7 weeks old) were purchased from Japan Clea Co. (Tokyo, Japan). Eight-week-old mice were used in the experiments. Food and water were given *ad libitum*. The mice were allotted into three groups: a control group ($n = 5$), a low-dose dendrimer-treated group ($n = 5$) and a high-dose dendrimer-treated group ($n = 5$). The mice were housed in plastic cages under controlled environmental conditions (temperature, $22 \pm 0.5\,^{\circ}C$; humidity, $50 \pm 5\%$; lights on 07:00–19:00 h). The experimental protocols were approved by the Ethics Committee of the Animal Care and Experimentation Council of the National Institute for Environmental Studies (NIES), Japan.

2.4. Administration of dendrimers

The intranasal route is widely used for the administration of pharmaceutical agents and vaccines. We considered a single intranasal instillation dose of 15 μg to be a "high dose" and 3 μg to be a "low dose" of dendrimers in the present study.

The mice were treated with a single dose of 30 μL PAMAM dendrimers (3 or 15 μg/mouse) into both nostrils under light sodium pentobarbital anesthesia. The control mice were given ultrapure water only.

2.5. Serum biochemical assay

Twenty-four hours after the intranasal instillation of PAMAM dendrimers, blood was drawn from the heart of each mouse under deep sodium pentobarbital anesthesia to examine various biochemical markers. The blood urea nitrogen (BUN), creatinine (CRE), total cholesterol (T-CHO), triglyceride (TG), pyruvic acid (PA), and lactic acid (LA) levels were analyzed using enzymatic methods, while the sodium (Na) and potassium (K) levels were analyzed using ion electrode methods. Then, the calcium (Ca) and iron (Fe) levels were analyzed using colorimetric assays, and the aspartate transaminase (AST), alanine transaminase (ALT), and lactate dehydrogenase (LDH) levels were analyzed using enzyme activity assays.

2.6. Microarray analyses and bioinformatics

To detect gene expression changes in the olfactory bulb, hippocampus, and cerebral cortex after a single intranasal instillation of dendrimers, microarray analyses were performed using an Agilent microarray (SurePrint G3 8×60 K mouse; Agilent Technologies, Inc., Santa Clara, CA, USA). An equivalent amount of total RNAs from six mice were pooled from each group and were used for microarray analyses. The arrays were hybridized and scanned in accordance with the manufacturer's directions at the facility of Hokkaido System Science Co., Ltd. (Sapporo, Japan). The expression values were normalized according to a median of 75%, filtered with a flag tag to remove genes which expression levels were low, and statistically analyzed using GeneSpring GX12.01 software (Agilent Technologies). Alterations in gene expression were represented as the $\log_2$ ratio. Finding pathways that integrated the collected biological knowledge were also analyzed using the GeneSpring software. Microarray data was submitted to GEO (Gene Expression Omnibus in National Center for Biotechnology Information, http://www.ncbi.nlm.nih.gov/geo/) and was registered as GSE56159.

2.7. Quantification of mRNA expression levels

Twenty-four hours after dendrimer instillation, the mice were sacrificed under deep pentobarbital anesthesia and the olfactory bulb, hippocampus, and cerebral cortex were collected from each group of mice and frozen quickly in liquid nitrogen, then stored at $-80\,^{\circ}C$ until the total RNA was extracted. Briefly, total RNA extraction from the tissue samples was performed using the BioRobot EZ-1 and EZ-1 RNA tissue mini-kits (Qiagen GmbH, Hilden, Germany). Then, the purity of the total RNA

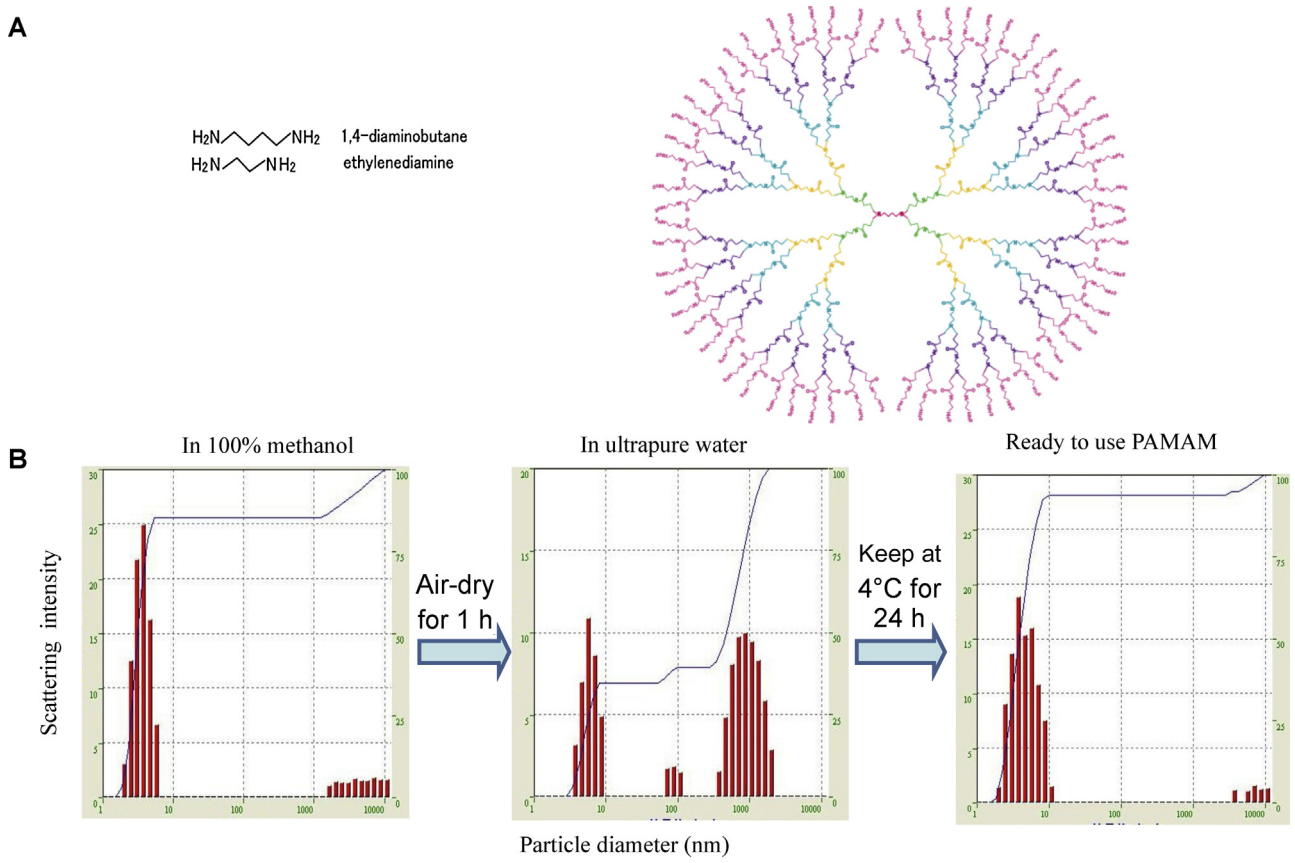

Fig. 1. (A) Schematic diagram of PAMAM dendrimer-NH_2 (G4) used in the present study and (B) distribution of hydrodynamic diameter of PAMAM dendrimer-NH_2 in ultrapure water. The particle size distributions were calculated using the light intensity distribution data. For the measurements, the whole range of operations from the detection of scattered light intensity distribution patterns to the calculation of the particle size distribution was performed. First, we measured the particle size distribution of PAMAM in 100% methanol; after the removal of methanol by air drying, the PAMAM dendrimers were again distributed in ultrapure water. Then, PAMAM was stored in ultrapure water overnight at 4 °C to allow the thorough dispersal of the PAMAM dendrimers, which were then used for the intranasal instillation experiments.

was examined, and the quantity was estimated using the ND-1000 NanoDrop RNA Assay protocol (NanoDrop, Wilmington, DE, USA), as described previously (Win-Shwe et al., 2008b). Next, we performed first-strand cDNA synthesis from the total RNA using SuperScript RNase H⁻ Reverse Transcriptase II (Invitrogen, USA), according to the manufacturer's protocol. We examined the mRNA expressions using a quantitative real-time RT-PCR method and the Applied Biosystems (ABI) Prism 7000 Sequence Detection System (Applied Biosystems Inc., Foster City, CA, USA). The tissue 18S rRNA level was used as an internal control. Some primers (cyclooxygenase 2 [COX2], NM_011198; heme oxygenase [HO] 1, NM_010442; interleukin [IL-1] β, NM_008361; nuclear factor kappa B [NFκB], NM_025937; and brain-derived neurotrophic factor [BDNF], NM_007540) were purchased from Qiagen, Sample & Assay Technologies. Other primers were designed in our laboratory: 18S (forward 5′-TACCACATCCAAGAAGGCAG-3′, reverse 5′-TGCCCTCCAATGGATCCTC-3′), and nerve growth factor [NGF] (forward 5′-TGGGCTTCAGGGACAGAGTC-3′, reverse 5′-CAGCTTTCTATACTGGCCGCAG-3′). Data were analyzed using the comparative threshold cycle method. The relative mRNA expression levels were expressed as mRNA signals per unit of 18S rRNA (Rn18s) expression.

2.8. Preparation of histological brain slices

Twenty-four hours after dendrimer instillation, the brains were removed from two mice in each of the control and high-dose exposure groups after the animals had been deeply anesthetized with sodium pentobarbital; the brains were then fixed with 10% formalin. The fixed brains were dehydrated using a graded series of ethanol, cleared with xylene, and embedded in paraffin. Coronal paraffin sections were cut at a thickness of 4 μm using a microtome and were mounted on 3-aminopropyltriethoxysilane-coated glass slides and stained with hematoxylin and eosin (H&E) for histological examination.

2.9. Statistical analysis

All the data were expressed as the mean ± standard error (S.E.). The statistical analysis was performed using the StatMate II statistical analysis system for Microsoft Excel, Version 5.0 (Nankodo Inc., Tokyo, Japan). The dose-response data were analyzed using a one-way analysis of variance with a *post hoc* analysis using the Bonferroni/Dunn method. Differences were considered significant at $P < 0.05$.

3. Results

3.1. Serum biochemical markers

Standard serum biochemical markers were monitored after acute PAMAM dendrimer treatment. The BUN, CRE, Na, K, Fe, AST, ALT, LDH, T-CHO, TG, PA, and LA levels did not differ significantly between the control and the dendrimer-treated mice (Table 1). These findings indicate that no general toxicity was observed in the present study.

3.2. Microarray analyses

2506 to 5027 genes with $\log_2$ fold changes >1.5 or <−1.5 from the three brain areas were selected and analyzed by the SEA (Single Experiment Analysis) of Genespring to find matching genes out of functional pathways in Wikipathway which was downloaded into GeneSpring database. The SEA pathway analysis can find functional annotation pathway listed by those matching genes between experimental data and genes in the known pathway of Wikipathway. The pathway analysis showed pluripotent network, serotonin-anxiety pathway, TGF-beta receptor signaling, prostaglandin synthesis-regulation, complement-coagulation cascades, blood coagulation cascade and chemokine-signaling pathway and non-odorant GPCR signaling pathways among a more than 1.5-fold up-regulation or

Table 1
Standard serum biochemical markers from dendrimer-treated mice.

	BUN (mg/dL)	CRE (mg/dL)	Na (mEq/L)	K (mEq/L)	Fe (μg/dL)	AST (IU/L)	ALT (IU/L)	LDH (IU/L)	T-CHO (mg/dL)	TG (mg/dL)	PA (mg/dL)	LA (mg/dL)
Control	13.8 ± 4.2	0.05 ± 0.0	150.0 ± 24.7	3.1 ± 0.7	78.2 ± 30.3	58.2 ± 33.6	17.8 ± 6.7	187.8 ± 82.3	29.8 ± 9.8	48.6 ± 26.7	0.23 ± 0.1	20.1 ± 6.2
Low dose	14.5 ± 4.5	0.05 ± 0.0	162.8 ± 2.2	2.8 ± 1.0	68.4 ± 24.8	45.6 ± 15.8	19.0 ± 5.6	171.8 ± 54.1	29.8 ± 14.2	31.4 ± 13.0	0.12 ± 0.1	16.2 ± 12.0
High dose	19.4 ± 6.4	0.08 ± 0.1	164.0 ± 1.2	3.3 ± 0.8	68.2 ± 24.3	48.2 ± 9.6	21.4 ± 1.0	170.2 ± 22.2	38.8 ± 15.0	50.8 ± 19.5	0.12 ± 0.3	28.3 ± 24.2

Data represents the mean ± SD ($n = 5$ from each group).
Abbreviations: blood urea nitrogen; BUN; creatinine; CRE; sodium; Na; potassium; K; iron; Fe; aspartate transaminase; AST; alanine transaminase, ALT; lactate dehydrogenase, LDH; total cholesterol, T-CHO, triglyceride, TG; pyruvic acid, PA; lactic acid, LA.

Table 2
Functional annotation pathway listed by pathway analysis that found matching genes between experimental data and genes in the known pathway of Wikipathway.

Tissues	Functional annotated pathways of Wikipathway	*P*-value	Matched gene entities	Gene entities in the pathway
Olfactory bulb	Mm_PluriNetWork_WP1763_41345	0.00150	12	291
	Mm_serotonin_and_anxiety_WP2141_47355	0.00192	3	18
	Mm_TGF-beta_Receptor_Signaling_Pathway_WP258_41259	0.00192	8	150
	Mm_Alpha6-Beta4_Integrin_Signaling_Pathway_WP488_41271	0.00326	5	67
	Mm_ErbB_signaling_pathway_WP1261_41378	0.00486	4	46
	Mm_EGFR1_Signaling_Pathway_WP572_41396	0.00493	8	176
	Mm_Insulin_Signaling_WP65_41286	0.00945	7	159
Cerebral Cortex	Mm_Prostaglandin_Synthesis_and_Regulation_WP374_41394	0.00000	12	31
	Mm_Complement_and_Coagulation_Cascades_WP449_41301	0.00000	13	62
	Mm_PluriNetWork_WP1763_41345	0.00025	28	291
	Mm_metapathway_biotransformation_WP1251_41349	0.00069	16	143
	Mm_Eicosanoid_Synthesis_WP318_41263	0.00149	5	19
	Mm_Monoamine_GPCRs_WP570_48232	0.00386	6	33
	Mm_TGF-beta_Receptor_Signaling_Pathway_WP258_41259	0.00458	15	150
	Adherens junction	0.00478	3	8
	Mm_Androgen_Receptor_Signaling_Pathway_WP252_47768	0.00577	12	112
	Mm_Nuclear_Receptors_WP509_41291	0.00789	6	38
Hippocampus	Mm_Chemokine_signaling_pathway_WP2292_53116	0.00010	16	193
	Mm_TGF_Beta_Signaling_Pathway_WP113_41270	0.00013	8	52
	Mm_Non-odorant_GPCRs_WP1396_41256	0.00013	20	267
	Mm_MAPK_signaling_pathway_WP493_47770	0.00086	13	159
	Mm_Type_II_interferon_signaling_(IFNG)_WP1253_48389	0.00257	5	34
	Mm_Monoamine_GPCRs_WP570_48232	0.00257	5	33
	Mm_PluriNetWork_WP1763_41345	0.00562	17	291
	Mm_Insulin_Signaling_WP65_41286	0.00674	11	159
	Mm_Tryptophan_metabolism_WP79_47759	0.00819	5	44

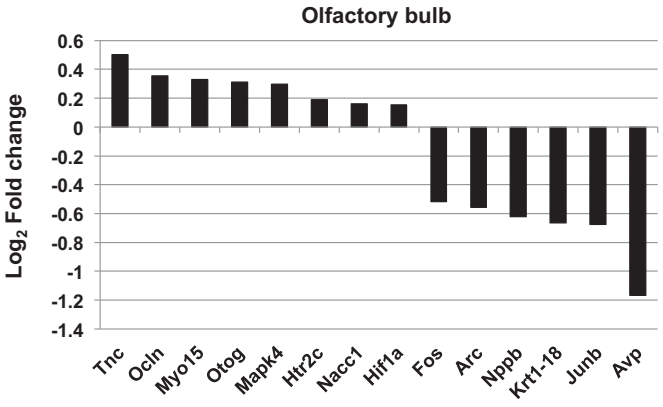

Fig. 2. Microarray analyses in the olfactory bulb. The relative mRNA expression was shown as the log fold-change referring to the control RNA level. Each bar represents a value of pooled RNAs from six mice per group.

down-regulation in the gene expression level (Table 2). Top 15–26 altered-gene expressions were shown in the olfactory bulb (Fig. 2), cerebral cortex (Fig. 3) and hippocampus (Fig. 4) of mice treated with high-dose dendrimers, compared with the levels in the control mice. Interestingly, pluripotent network and TGF-beta receptor signaling related-genes were commonly responsive among three brain areas by exposure to PAMAM dendrimers. In the hippocampus, we found that Mapk4, Bdnf and Htr2 C were up-regulated (Fig. 4A) and Bdnf-Mapk-related signaling pathway was expressed in Fig 4B.

3.3. Inflammatory markers and neurotrophins in the brain

To detect the inflammatory and immune responses after dendrimer treatment, we examined the gene expression levels of the potent inflammatory mediator *Cox2*, the oxidative stress marker *Ho1*, the immune cell cytokine *Il-1β*, and the transcription factor *NfκB* in the olfactory bulb, hippocampus, and cerebral cortex (Table 3). In addition, as we found that Bdnf expression was up-regulated in hippocampus in our microarray results, we also examined the expression levels of neurotrophins, such as *Ngf* and *Bdnf*, and found that the Bdnf mRNA levels were significantly increased in the hippocampus and cerebral cortex of the high-dose dendrimer-treated mice ($P < 0.05$, Fig. 5).

3.4. Histological findings

We examined the morphological and pathological changes in the olfactory bulb and hippocampus after a single exposure to dendrimers. We did not find any obvious significant changes in the brains of mice exposed to dendrimers, compared with the control group (data not shown).

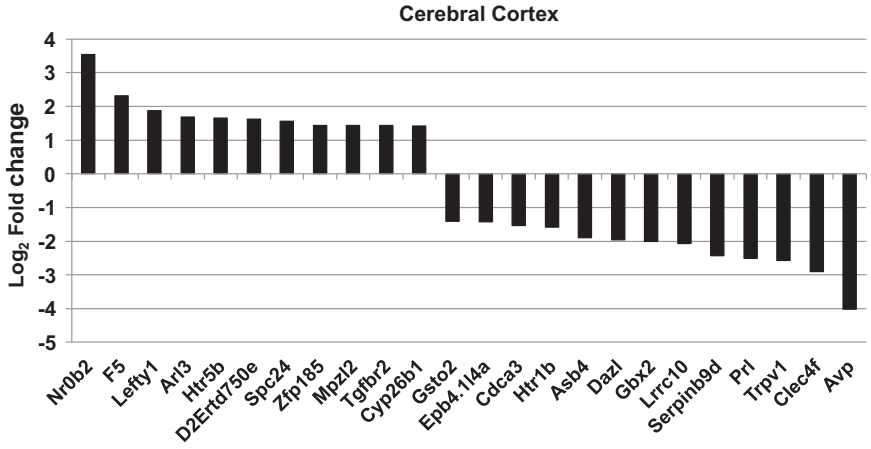

Fig. 3. Microarray analyses in the cerebral cortex. The relative mRNA expression was shown as the log fold-change referring to the control RNA level. Each bar represents a value of pooled RNAs from six mice per group.

Table 3
The relative mRNA expression level of inflammatory markers from dendrimer-treated mice.

Brain area	Dendrimers	*Cox2*	*Ho1*	*qIl1β*	*NfκB*
Olfactory bulb	Control	0.55 ± 0.11	1.40 ± 0.28	1.25 ± 0.82	1.15 ± 0.07
	Low dose	0.55 ± 0.13	1.42 ± 0.23	0.99 ± 0.25	1.35 ± 0.11
	High dose	0.43 ± 0.07	2.00 ± 0.76	1.12 ± 0.41	1.30 ± 0.08
Hippocampus	Control	1.01 ± 0.27	1.02 ± 0.90	0.64 ± 0.29	0.95 ± 0.16
	Low dose	0.87 ± 0.15	0.97 ± 0.11	0.38 ± 0.13	0.78 ± 0.13
	High dose	1.04 ± 0.23	1.24 ± 0.09	0.78 ± 0.28	0.96 ± 0.15
Cerebral cortex	Control	1.69 ± 1.08	1.08 ± 0.07	1.44 ± 0.62	1.05 ± 0.17
	Low dose	2.03 ± 0.85	1.13 ± 0.24	1.24 ± 0.36	1.03 ± 0.10
	High dose	1.58 ± 0.61	1.14 ± 0.14	1.15 ± 0.21	0.95 ± 0.15

Data are normalized for *Rn18s* mRNA levels and represents the mean ± SE ($n = 5$ from each group).
Abbreviations: cyclooxygenase 2; *Cox2*; heme oxygenase 1; *Ho1*; interleukin-1β; *Il1β*; nuclear factor kappa B; *NfκB*.

4. Discussion

The major findings of the present study were that pluripotent network and TGF-beta receptor signaling related-genes were commonly responsive among specific pathways with less than 0.01 of *P*-value in three brain areas by exposure to PAMAM dendrimers. Moreover, the increased expression level of Bdnf gene in the hippocampus and cerebral cortex of high-dose dendrimer-treated mice was observed. To detect the general toxicity of dendrimers, we examined serum biochemical markers and brain inflammatory biomarkers. The results showed that no remarkable changes were observed in the blood or brain. This was the first *in vivo* study to show that the administration of an acute single high dose of dendrimer causes mild effects on neurological gene expressions in the olfactory bulb, hippocampus and cerebral cortex.

Regarding the treatment of central nervous system diseases, it is important to understand the drug delivery system to the brain and to study the toxicity of drug-carrying dendrimers in the brain. There are many routes of administration to the brain, such as intraparenchymal, intraventricular, and subarachnoid injections. In the present study, we used intranasal instillation, which is relevant to human applications. A recent study showed that dendrimers are able to cross the cell membrane of primary neurons, as detected using confocal imaging, and are also able to diffuse to the CNS tissues after intraparenchymal or intraventricular injections (Albertazzi et al., 2013). The same group also demonstrated that the apoptotic cell death of neurons was induced by 100-nm of G4 PAMAM, but not in brain tissues by a sub-micromolar dose. Moreover, using zebra fish embryos, the developmental toxicity of low-generation G3.5 and G4 PAMAM dendrimers has been demonstrated (Heiden et al., 2007).

Some *in vitro* studies have demonstrated that the exposure of human hepatocellular carcinoma (HepG2) cells and human peripheral blood mononuclear cells (PBMCs) from healthy human volunteers to gold nanoparticles capped with PAMAM or sodium citrate (50 μM) might lead to the disturbance of cells, with cytotoxic effects and DNA damage (Paino et al., 2012).

In this study, a microarray analysis showed the up-regulation of the expression levels of genes related to pluripotent network, serotonin-anxiety pathway, TGF-beta receptor signaling, prostaglandin synthesis-regulation, complement-coagulation cascades, blood coagulation cascade and chemokine-signaling pathway and non-odorant GPCR signaling pathways in brain tissues. A trimethyltin-induced model of hippocampal dentate granule cell death dependent upon TNF receptor signaling were demonstrated elevations of TGFβ accompanied with other TNF related cytokines (Funk et al., 2011). Taken together, these results suggest that an acute dose of dendrimers may at least partly cause neuroinflammation and may affect some behavioral functions. Moreover, in the present study, our microarray results showed that Bdnf expression was up-regulated in the hippocampus. This is consistent with mRNA result. It has been reported that BDNF and its signaling pathway involving Akrt, MAPK and P70S6 K are potential target for environmental chemical-induced neurotoxicity (Fattori et al., 2008). BDNF is a neurotrophin and it affects survival and function of neurons in the central nervous system. The up-regulation of Bdnf expression in the present study may be due to body homeostasis, it is also suggested that BDNF-MAPK pathway may involve cellular proliferation, differentiation and inflammation and apoptosis in molecular mechanism.

Regarding the biodistribution of dendrimers, several studies have suggested that the olfactory nerve pathway should be

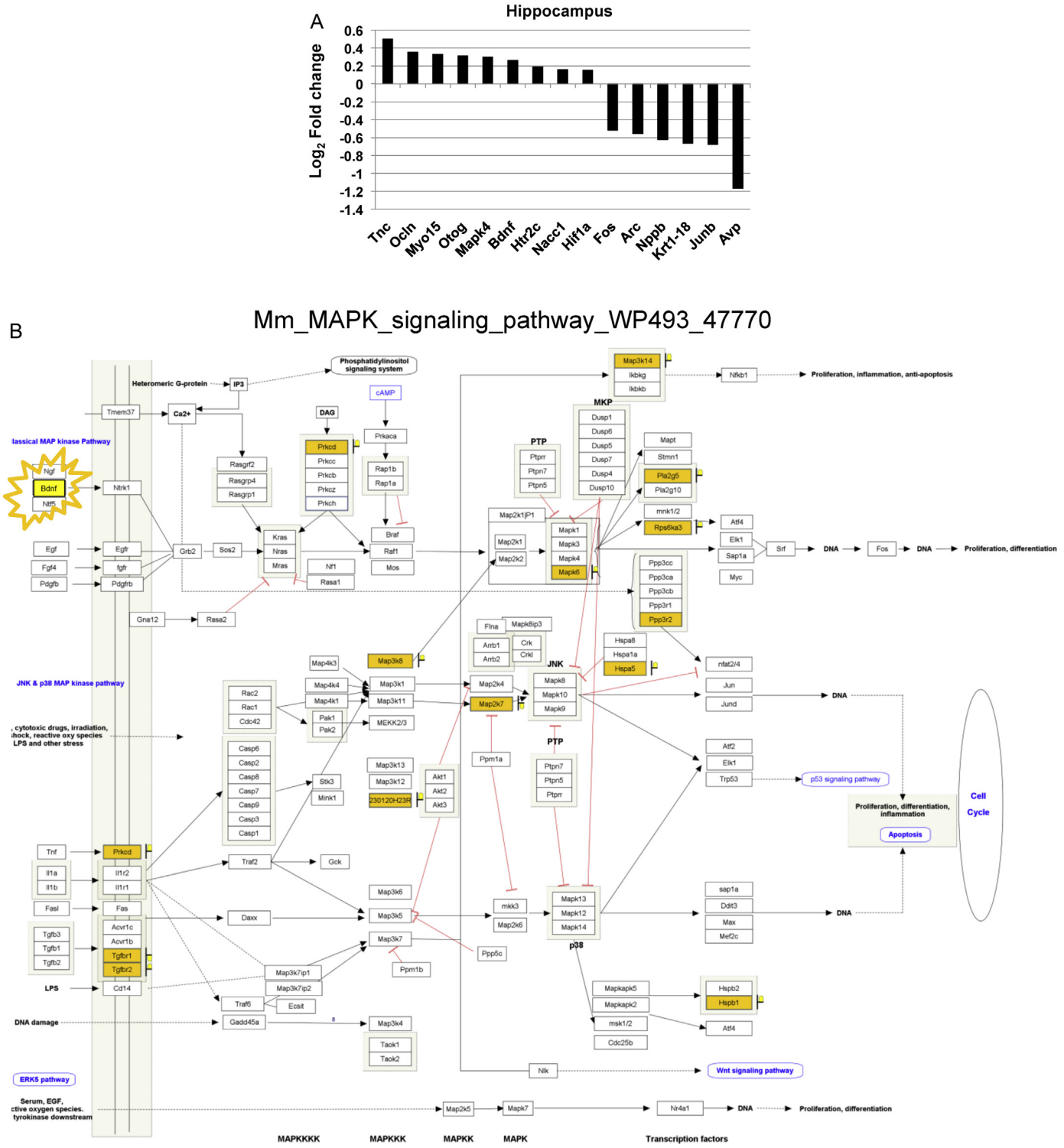

Fig. 4. (A) Microarray analyses in the hippocampus. The relative mRNA expression was shown as the log fold-change referring to the control RNA level. Each bar represents a value of pooled RNAs from six mice per group. (B) Altered gene expression induced by the PAMAM dendrimer exposure were mapped on the BDNF-MAPK signaling pathway in mice of the Wikipathway.

considered as a portal of entry to the central nervous system in humans who are environmentally or occupationally exposed to airborne NPs (Oberdörster et al., 2004; De Lorenzo, 1970; Tjälve et al., 1996). In a landmark study in 1970, De Lorenzo used ultrafine particles to demonstrate that, in squirrel monkeys, intranasally instilled Ag-coated colloidal Au particles (50 nm) translocate anterogradely in the axons of the olfactory nerves to the olfactory bulbs (De Lorenzo, 1970). It has also been shown that manganese (Mn), cadmium (Cd), nickel (Ni), and cobalt (Co) nanomaterials that come into contact with the olfactory epithelium can be transported to the brain *via* olfactory neurons (Tallkvist et al., 1998; Tjälve and Henriksson, 1999; Henriksson and Tjälve, 2000; Persson et al., 2003; Elder et al., 2006). Oberdörster and colleagues demonstrated that the inhalation of ultrafine elemental ^{13}C particles (36 nm)

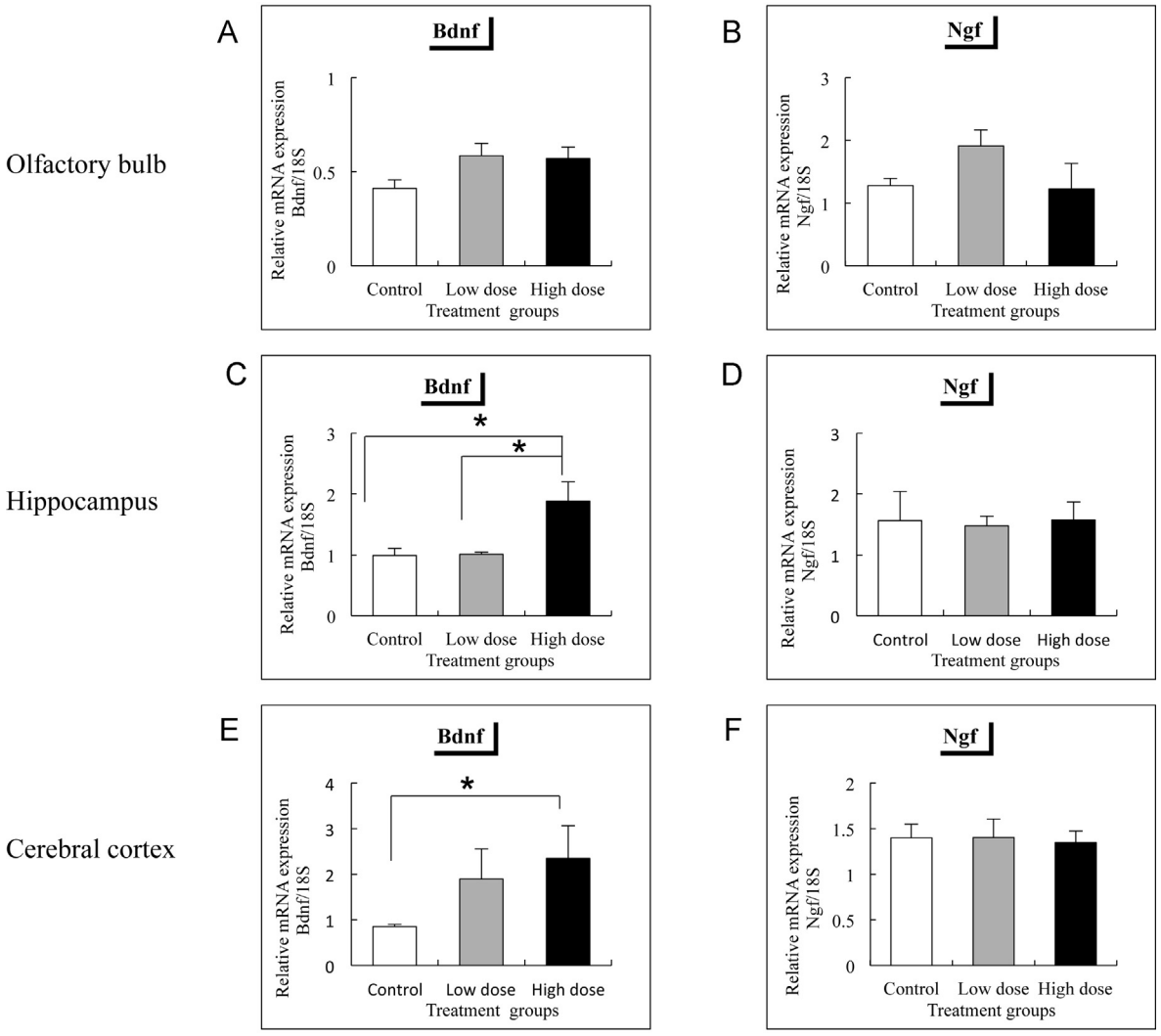

Fig. 5. mRNA expression of neurotrophins in dendrimer-treated mice (A–F). Each bar represents the mean ± SE ($n = 5$ from each group). *Abbreviations*: Brain-derived neurotrophic factor, *Bdnf*; nerve growth factor, *Ngf*. (A) and (B) show the expressions in the olfactory bulb; (C) and (D) show the expressions in the hippocampus; and (E) and (F) show the markers in the cerebral cortex.

by rats for 6 h in a whole-body exposure chamber led to a significant and persistent increase in the accumulation of ^{13}C NPs in the olfactory bulb on day 1 and that the NP concentration continued to increase up until day 7 (Oberdörster et al., 2004). The same study also showed that the concentrations of ^{13}C NPs were significantly increased in the cerebrum and cerebellum, but that the increase was inconsistent; that is, a significant difference was only observed on one additional day of the post-exposure period (day 1). Regarding the present study, we have no evidence that dendrimers translocate to the systemic circulation. However, Nemmar et al. (2002) reported that inhaled ultrafine technetium (^{99m}Tc)-labeled carbon particles translocate into the systemic circulation within 5 min by diffusion. The transport of nanoparticles across the blood–brain barrier (BBB) is reportedly possible by either passive diffusion or by carrier-mediated endocytosis (Hoet et al., 2004). A recent study using a BBB *in vitro* model showed that G4 PAMAM dendrimers were able to cross the BBB and induced CD11b and CCR2 overexpression in primary murine microglia (Bertero et al., 2014). In the present study, we observed fluorescent signals thought to represent dendrimers in the hippocampus. Thus, the intranasally instilled 4-nm PAMAM used in the present study might translocate to the brain *via* an olfactory nerve or the systemic circulation. The potential translocation routes for intranasally instilled dendrimers in the mouse brain are shown in Fig. 6. Although we could not identify the exact mechanism for the translocation of the dendrimers from the nose to the brain, drugs or molecules can reportedly be transported by two possible routes: a transporter-mediated route and paracellular transport (Frey, 2002; Thorne et al., 2004; Dhanda et al., 2005; Pardridge, 2005). Recently, an intranasal route *via* an epithelial permeabilizer has been shown to be capable of delivering drugs to the CNS (Krishan et al., 2014).

We have measured the size of PAMAM dendrimers in the original commercial solution [100% methanol (3.4 ± 0.9 nm)], in the ultrapure water (mean size is 5.7 ± 1.4 nm in first peak; 976 ± 391 nm in second peak) after removing methanol and after 24 h in the ultrapure water (5.6 ± 2.3 nm) to remove second peak of aggregation. Our results indicated that no much change of size and not much aggregation were observed before administration to animals.

Neurotrophins have been identified as targets for neurotoxicants and are known to play a role in bidirectional signaling between the cells of the immune and nervous systems. Bdnf is a primary neurotrophin in the hippocampus (Karaoulanis and Angelopoulos, 2010) and plays a key role in neuro-immune responses (Aloe et al., 1994). Moreover, multiple neurotransmitter systems, such as dopamine, glutamate, acetylcholine, and

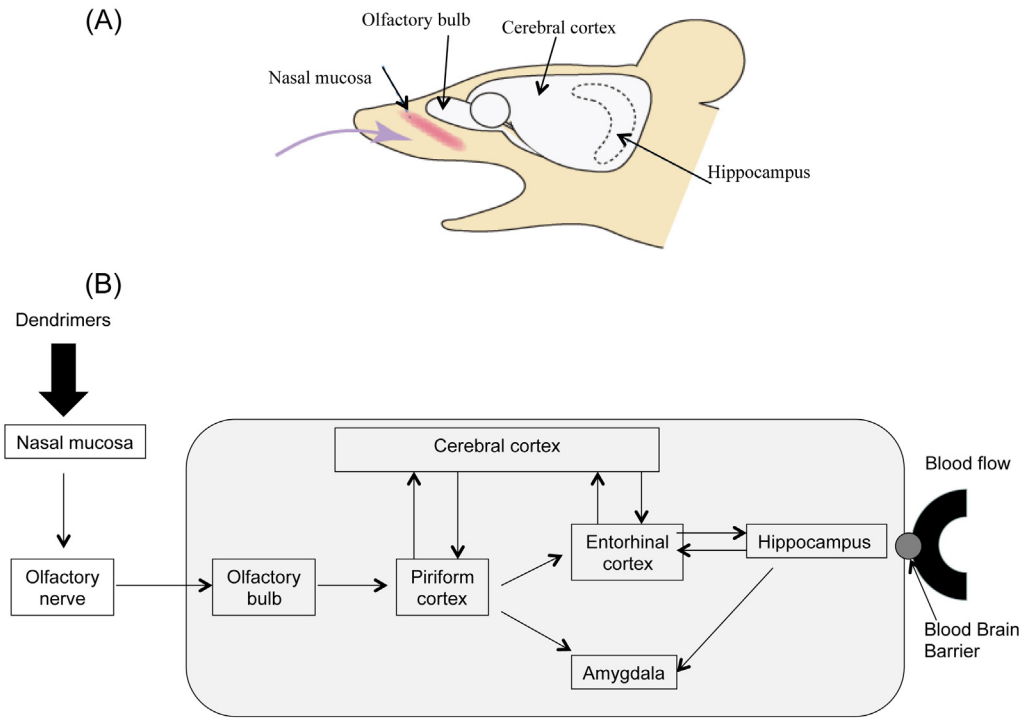

Fig. 6. Diagram showing the target brain regions of the mouse brain examined in the present study (A) and the potential translocation routes for intranasally instilled dendrimers in the mouse brain (B).

serotonin, also take part in proper neuronal functions. On the other hand, according to requirements, body homeostasis signals induce neurotrophin production in the brain. The balance between toxic substances and trophic substances secreted from microglia may influence neurotoxicity and neuroprotection. Finally, our present study indicates that dendrimers induce minor toxicity in the brain but that BDNF production compensates for this toxicity.

Based on our present findings, we suggest that PAMAM dendrimers appeared to be not toxic in general; however, the expressions of some neurological-related genes were induced by high-dose treatment. Although we observed the effects of dendrimers at one time point in the present study, time points that are relevant to the PAMAM pharmacokinetics should also be examined. The cytotoxicity and cell permeability of PAMAM dendrimers depend upon the concentration and generation of the dendrimers (Jevprasesphant et al., 2003). Furthermore, cytotoxicity may be related to the radius of gyration, the molecular shape, and the dimensions of a particular dendrimer (Metullio et al., 2004). A recent report indicated that dendrimer toxicity was mainly due to its outer surface layer and that the toxicity could be manipulated by modifying the surface layer (Chauhan et al., 2010). We suggest that the route of administration (*e.g.*, intranasal, intravenous, intratracheal, or intraperitoneal), dosage (low or high dose), and duration of treatment (acute, subchronic, chronic, or intermittent) may also influence the toxicological and pharmacological effects of dendrimers *in vivo*. Further studies are needed to explore the time course effects of dendrimers on biodistribution and the effects of various exposure routes and durations on dendrimer toxicity.

Conflict of interest

The authors declare that there are no conflicts of interest.

Transparency document

The Transparency document associated with this article can be found in the online version.

Acknowledgment

This work was funded by a by Grant-in-Aid for Scientific Research from the Ministry of Education, Science, Culture and Sports of Japan (24241013) to H.S. We thank Ms. Hiroko Nansai, Ryoko Yanagisawa and Naoko Ueki for their technical assistance.

References

Albertazzi, L., Gherardini, L., Brondi, M., Sulis, Sato, S., Bifone, A., Pizzorusso, T., Ratto, G.M., Bardi, G., 2013. In vivo distribution and toxicity of PAMAM dendrimers in the central nervous system depend on their surface chemistry. Mol. Pharm. 10, 249–260.

Aloe, L., Skaper, S.D., Leon, A., Levi-Montalcini, R., 1994. Nerve growth factor and autoimmune diseases. Autoimmunity 19, 141–150.

Bertero, A., Boni, A., Gemmi, M., Gagliardi, M., Bifone, A., Bardi, G., 2014. Surface functionalisation regulates polyamidoamine dendrimer toxicity on blood–brain barrier cells and the modulation of key inflammatory receptors on microglia. Nanotoxicology 8, 158–168.

Buhleier, E., Wehner, W., Vogtle, F., 1978. Cascade and nonskid-chain-like synthesis of molecular cavity topologies. Synthesis 2, 155–158.

Chauhan, A.S., Jain, N.K., Diwan, P.V., 2010. Pre-clinical and behavioural toxicity profile of PAMAM dendrimers in mice. Proc R Soc A, http://dx.doi.org/10.1098/rspa.2009.0448.

Cho, W.S., Kang, B.C., Lee, J.K., Jeong, J., Che, J.H., Seok, S.H., 2013. Comparative absorption, distribution, and excretion of titanium dioxide and zinc oxide nanoparticles after repeated oral administration. Part Fibre Toxicol. 10, 9.

De Lorenzo, A.J.D., 1970. The olfactory neuron and the blood–brain barrier. In: Wolstenholme, G.E.W., Knight, J. (Eds.), Taste and Smell in Vertebrates. J. & A. Churchill, London, UK, pp. 151–176.

Dear, J.W., Kobayashi, H., Brechbiel, M.W., Star, R.A., 2006. Imaging acute renal failure with polyamine dendrimer-based MRI contrast agents. Nephron. Clin. Pract. 103, c45–c49.

Dhanda, D.S., Frey, I.I.W.H., Leopold, D., et al., 2005. Approaches for drug deposition in the human olfactory epithelium. Drug Del. Tech. 5, 64–72.

Elder, A., Gelein, R., Silva, V., Feikert, T., Opanashuk, L., Carter, J., Potter, R., Maynard, A., Ito, Y., Finkelstein, J., Oberdorster, G., 2006. Translocation of inhaled ultrafine manganese oxide particles to the central nervous system. Environ. Health Perspect. 114, 1172–1178.

Fattori, V.AbeS., Kobayashi, K., Costa, L.G., Tsuji, R., 2008. Effects of postnatal ethanol exposure on neurotrophic factors and signal transduction pathways in rat brain. J. Appl. Toxicol. 28, 370–376.

Frey, I.I.W.H., 2002. Bypassing the blood–brain barrier to delivery therapeutic agents to the brain and spinal cord. Drug Del. Tech. 2, 46–49.

Funk, J.A., Gohlke, J., Kraft, A.D., McPherson, C.A., Collins, J.B., Jean Harry, G., 2011. Voluntary exercise protects hippocampal neurons from trimethyltin injury: possible role of interleukin-6 to modulate tumor necrosis factor receptor-mediated neurotoxicity. Brain Behav. Immun. 25, 1063–1077.
Heiden, T.C., Dengler, E., Kao, W.J., Heideman, W., Peterson, R.E., 2007. Developmental toxicity of low generation PAMAM dendrimers in zebrafish. Toxicol. Appl. Pharmacol. 225, 70–79.
Henriksson, J., Tjälve, H., 2000. Manganese taken up into the CNS via the olfactory pathway in rats affects astrocytes. Toxicol. Sci. 55, 392–398.
Hoet, P.H., Brüske-Hohlfeld, I., Salata, O.V., 2004. Nanoparticles – known and unknown health risks. J. Nanobiotechnol. 2, 12.
Hong, S., Bielinska, A.U., Mecke, A., Keszler, B., Beals, J.L., Shi, X., Balogh, L., Orr, B.G., Baker Jr., J.R., Banaszak Holl, M.M., 2004. Interaction of poly(amidoamine) dendrimers with supported lipid bilayers and cells: hole formation and the relation to transport. Bioconjug. Chem. 15, 774–782.
Jevprasesphant, R., Penny, J., Jalal, R., Attwood, D., McKeown, N.B., D'Emanuele, A., 2003. The influence of surface modification on the cytotoxicity of PAMAM dendrimers. Int. J. Pharm. 252, 263–266.
Karaoulanis, S.E., Angelopoulos, N.V., 2010. The role of immune system in depression. Psychiatrike 21, 17–30.
Krishan, M., Gudelsky, G.A., Desai, P.B., Genter, M.B., 2014. Manipulation of olfactory tight junctions using papaverine to enhance intranasal delivery of gemcitabine to the brain. Drug Deliv. 21, 8–16.
Lee, C.C., MacKay, J.A., Fréchet, J.M., Szoka, F.C., 2005. Designing dendrimers for biological applications. Nat. Biotechnol. 23, 1517–1526.
Lee, J.H., Cha, K.E., Kim, M.S., Hong, H.W., Chung, D.J., Ryu, G., Myung, H., 2009. Nanosized polyamidoamine (PAMAM) dendrimer-induced apoptosis mediated by mitochondrial dysfunction. Toxicol. Lett. 190, 202–207.
Leroueil, P.R., Berry, S.A., Duthie, K., Han, G., Rotello, V.M., McNerny, D.Q., Baker Jr., J.R., Orr, B.G., Holl, M.M., 2008. Wide varieties of cationic nanoparticles induce defects in supported lipid bilayers. Nano. Lett. 8, 420–424.
Mukherjee, S.P., Davoren, M., Byrne, H.J., 2010a. In vitro mammalian cytotoxicological study of PAMAM dendrimers – towards quantitative structure activity relationships. Toxicol. In Vitro 24, 169–177.
Mukherjee, S.P., Lyng, F.M., Garcia, A., Davoren, M., Byrne, H.J., 2010b. Mechanistic studies of in vitro cytotoxicity of poly(amidoamine) dendrimers in mammalian cells. Toxicol. Appl. Pharmacol. 248, 259–268.
Metullio, L., Ferrone, M., Coslanich, A., Fuchs, S., Fermeglia, M., Paneni, M.S., Pricl, S., 2004. Polyamidoamine (Yet Not PAMAM) dendrimers as bioinspired materials for drug delivery: structure-activity relationships by molecular simulations. Biomacromolecules 5, 1371–1378.
Na, M., Yiyun, C., Tongwen, X., Yang, D., Xiaomin, W., Zhenwei, L., Zhichao, C., Guanyi, H., Yunyu, S., Longping, W., 2006. Dendrimers as potential drug carriers Part II. Prolonged delivery of ketoprofen by in vitro and in vivo studies. Eur. J. Med. Chem. 41, 670–674.
Naha, P.C., Davoren, M., Casey, A., Byrne, H.J., 2009. An ecotoxicological study of poly(amidoamine) dendrimers-toward quantitative structure activity relationships. Environ. Sci. Technol. 43, 6864–6869.
Naha, P.C., Davoren, M., Lyng, F.M., Byrne, H.J., 2010. Reactive oxygen species (ROS) induced cytokine production and cytotoxicity of PAMAM dendrimers in J774A.1 cells. Toxicol. Appl. Pharmacol. 246, 91–99.
Nemmar, A., Hoet, P.H., Vanquickenborne, B., Dinsdale, D., Thomeer, M., Hoylaerts, M.F., Vanbilloen, H., Mortelmans, L., Nemery, B., 2002. Passage of inhaled particles into the blood circulation in humans. Circulation 105, 411–414.
Newkome, G.R., Yao, Z.Q., Baker, G.R., Gupta, V.K., 1985. Cascade molecules: a new approach to micelles A [27]-arborol. J. Org. Chem. 50, 2003–2006.
Oberdörster, G., Sharp, Z., Atudorei, V., Elder, A., Gelein, R., Kreyling, W., Cox, C., 2004. Translocation of inhaled ultrafine particles to the brain. Inhal. Toxicol. 16, 437–445.
Paino, I.M., Marangoni, V.S., de Oliveira Rde, C., Antunes, L.M., Zucolotto, V., 2012. Cyto and genotoxicity of gold nanoparticles in human hepatocellular carcinoma and peripheral blood mononuclear cells. Toxicol. Lett. 215, 119–125.
Pardridge, W.M., 2005. The blood–brain barrier and neurotherapeutics. NeuroRx 2, 1–2.
Persson, E., Henriksson, J., Tjälve, H., 2003. Uptake of cobalt from the nasal mucosa into the brain via olfactory pathways in rats. Toxicol. Lett. 145, 19–27.
Pushkar, S., Philip, A., Pathak, K., Pathak, D., 2006. Dendrimers: nanotechnology derived novel polymers in drug delivery. Indian J. Pharm. Educ. Res. 40, 153–158.
Swanson, S.D., Kukowska-Latallo, J.F., Patri, A.K., Chen, C., Ge, S., Cao, Z., Kotlyar, A., East, A.T., Baker, J.R., 2008. Targeted gadolinium-loaded dendrimer nanoparticles for tumor-specific magnetic resonance contrast enhancement. Int. J. Nanomed. 3, 201–210.
Tallkvist, J., Henriksson, J., d'Argy, R., Tjälve, H., 1998. Transport and subcellular distribution of nickel in the olfactory system of pikes and rats. Toxicol. Sci. 43, 196–203.
Tekade, R.K., Kumar, P.V., Jain, N.K., 2009. Dendrimers in oncology: an expanding horizon. Chem. Rev. 109, 49–87.
Thorne, R.G., Pronk, G.J., Padmanabhan, V., Frey, W.H.I.I., 2004. Delivery of insulin-like growth factor-I to the rat brain and spinal cord along olfactory and trigeminal pathways following intranasal administration. Neuroscience 127, 481–496.
Tjälve, H., Henriksson, J., Tallkvist, J., Larsson, B.S., Lindquist, N.G., 1996. Uptake of manganese and cadmium from the nasal mucosa into the central nervous system via olfactory pathways in rats. Pharmacol. Toxicol. 79, 347–356.
Tjälve, H., Henriksson, J., 1999. Uptake of metals in the brain via olfactory pathways. Neurotoxicology 20, 181–196.
Tomalia, D.A., Baker, H., Dewald, J., Hall, M., Kallos, G., Martin, S., Roeck, J., Ryder, J., Smith, P., 1985. A new class of polymers: starburst-dendritic macromolecules. Polym. J. 17, 117–132.
Win-Shwe, T.T., Yamamoto, S., Ahmed, S., Kakeyama, M., Kobayashi, T., Fujimaki, H., 2006. Brain cytokine and chemokine mRNA expression in mice induced by intranasal instillation with ultrafine carbon black. Toxicol. Lett. 163, 153–160.
Win-Shwe, T.T., Yamamoto, S., Fujitani, Y., Hirano, S., Fujimaki, H., 2008a. Spatial learning and memory function-related gene expression in the hippocampus of mouse exposed to nanoparticle-rich diesel exhaust. Neurotoxicology 29, 940–947.
Win-Shwe, T.T., Mitsushima, D., Yamamoto, S., Fukushima, A., Funabashi, T., Kobayashi, T., Fujimaki, H., 2008b. Changes in neurotransmitter levels and proinflammatory cytokine mRNA expressions in the mice olfactory bulb following nanoparticle exposure. Toxicol. Appl. Pharmacol. 15, 192–198.
Win-Shwe, T.T., Mitsushima, D., Yamamoto, S., Fujitani, Y., Funabashi, T., Hirano, S., Fujimaki, H., 2009. Extracellular glutamate level and NMDA receptor subunit expression in mouse olfactory bulb following nanoparticle-rich diesel exhaust exposure. Inhal. Toxicol. 21, 828–836.
Win-Shwe, T.T., Fujimaki, H., 2011. Nanoparticles and neurotoxicity. Int. J. Mol. Sci. 12, 6267–6280.
Win-Shwe, T.T., Yamamoto, S., Fujitani, Y., Hirano, S., Fujimaki, H., 2012a. Nanoparticle-rich diesel exhaust affects hippocampal-dependent spatial learning and NMDA receptor subunit expression in female mice. Nanotoxicology 6, 543–553.
Win-Shwe, T.T., Fujimaki, H., Fujitani, Y., Hirano, S., 2012b. Novel object recognition ability in female mice following exposure to nanoparticle-rich diesel exhaust. Toxicol. Appl. Pharmacol. 262, 355–362.
Ze, Y., Zheng, L., Zhao, X., Gui, S., Sang, X., Su, J., Guan, N., Zhu, L., Sheng, L., Hu, R., Cheng, J., Cheng, Z., Sun, Q., Wang, L., Hong, F., 2013. Molecular mechanism of titanium dioxide nanoparticles-induced oxidative injury in the brain of mice. Chemosphere 92, 1183–1189.
Zhou, J., Wu, J., Hafdi, N., Behr, J.P., Erbacher, P., Peng, L., 2006. PAMAM dendrimers for efficient siRNA delivery and potent gene silencing. Chem. Commun. (Camb). 22, 2362–2364.